Am J Transl Res 2025;17(7):5385-5397
www.ajtr.org /ISSN:1943-8141/AJTR0165033

Original Article

Extratumoral signs on mammography as a novel prognostic indicator for breast cancer: evidence from malignant nonspiculate and noncalcified masses

Ye Xu[1], Fei Wang[1], Dongbo Wu[1], Xinghua Liang[2], Jianghong Sun[1], Xiushi Zhang[1]

[1]*Department of Radiology, Harbin Medical University Cancer Hospital, Harbin, Heilongjiang, China;* [2]*Department of Radiology, Heilongjiang University Hospital, Harbin, Heilongjiang, China*

Received April 3, 2025; Accepted June 28, 2025; Epub July 15, 2025; Published July 30, 2025

Abstract: Objectives: To evaluate the prognostic significance of extratumoral structural abnormalities associated with malignant nonspiculate and noncalcified masses (NSNCMs) detected on mammography. Methods: Data from 354 breast cancer patients with mammographically detected NSNCMs between December 2017 and December 2018 were retrospectively analyzed. Cox regression analysis was performed to assess the impact of mammographic findings, particularly extratumoral structural abnormalities such as parenchymal and trabecular signs, on progression-free survival (PFS). Additionally, Kaplan-Meier survival curves were used for risk stratification. Results: The median follow-up period was 74 months (range: 10-83 months). Disease progression occurred in 122 patients (34.5%). Cox regression analysis revealed that among the mammographic features, the extratumoral contraction sign [hazard ratio (HR) = 2.56, 95% confidence interval (CI): 1.60-4.09, P < 0.001] and the extratumoral parallel sign (HR = 2.71, 95% CI: 1.57-4.70, P < 0.001) were independent predictors of NSNCM progression, demonstrating strong prognostic performance. In contrast, tumor signs did not show significant predictive value. Kaplan-Meier analysis further confirmed that these two extratumoral features effectively stratified the risk of progression in patients with malignant NSNCMs. Additionally, lymph node metastasis (HR = 2.37, 95% CI: 1.64-3.42, *P* < 0.001) and histological grade (HR = 2.03, 95% CI: 1.05-3.92, *P* = 0.036) were also identified as independent predictors of disease progression. Conclusions: Specific extratumoral structural abnormalities and their subclassifications on mammography are independent prognostic indicators in breast cancer patients with malignant NSNCMs. These findings provide an important basis for personalized treatment strategies in clinical practice.

Keywords: Breast cancer, progression-free survival, nonspiculate and noncalcified masses, extratumoral structural abnormalities, mammography

Introduction

Globally, approximately 2 million individuals are diagnosed with breast cancer each year, making it a leading cause of cancer-related mortality among women [1-3]. Disease progression is a major contributor to breast cancer deaths, significantly shortening patient survival. Accurate prediction of disease progression is therefore critical for effective management, enabling early identification of high-risk cases and optimization of treatment strategies to potentially prolong survival and improve quality of life.

The substantial heterogeneity of breast cancer poses significant challenges for prognostic prediction. Compared with clinicopathological features, imaging features provide a more intuitive and non-invasive assessment of systemic involvement and tumor burden, offering reproducible and easily applicable evaluations. In recent years, mammography has become an essential tool for breast tumor diagnosis [4, 5]. However, previous studies have primarily focused on microcalcifications and tumor-specific characteristics [6-9]. Critical gaps remain in the evaluation of nonspiculate and noncalcified masses (NSNCMs), which appear as masses

https://doi.org/10.62347/ETGF1320

lacking spiculated margins or internal calcifications on mammography. These lesions are generally considered to have a favorable prognosis due to the absence of imaging features typically associated with malignancy. Nonetheless, clinical observations have shown that malignant NSNCMs can still demonstrate varying degrees of disease progression.

Our previous study highlighted the value of extratumoral signs in distinguishing between benign and malignant breast lesions [10]. Building upon these findings, investigating the relationship between extratumoral structural abnormalities and poor prognosis in malignant NSNCMs holds substantial research significance.

Therefore, this study aimed to evaluate the association between extratumoral structural abnormalities on mammography and disease progression in malignant NSNCMs, and to determine whether these imaging features can serve as independent prognostic predictors alongside traditional clinicopathological factors. Our findings may facilitate the early identification of high-risk patients, enabling timely administration of adjuvant therapies to improve survival outcomes.

Materials and methods

Ethics statement

This observational study was approved by the Institutional Review Board of Harbin Medical University Cancer Hospital, which waived the requirement for informed consent due to the retrospective nature of the research and the use of routinely collected mammograms and clinical-pathological data (Approval ID: KY2024-04).

Patient selection

Data from hospitalized patients who underwent mammography at Harbin Medical University Cancer Hospital between December 2017 and December 2018 and were subsequently pathologically diagnosed with invasive ductal carcinoma were retrospectively analyzed. Cases identified as “nonspiculate, noncalcified mass” on the Picture Archiving and Communication System (PACS) were included.

Inclusion criteria: Patients were eligible if they: (1) Were subsequently pathologically diagnosed with invasive ductal carcinoma; (2) Had mammographic findings classified as malignant NSNCMs.

Exclusion criteria: Patients were excluded if they: (1) Were male; (2) Had a history of local mastectomy prior to mammography; (3) Had undergone breast biopsy or neoadjuvant therapy before mammography examination; (4) Had multiple breast lesions; (5) Had tumors that were not fully captured on imaging or mammograms that did not meet diagnostic standards; (6) Had incomplete clinical or pathological data; (7) Were lost to follow-up; (8) Were diagnosed with primary malignant tumors of other organs during follow-up.

Detailed inclusion and exclusion criteria and patient selection flow are presented in **Figure 1**. A total of 354 patients meeting these criteria were included in the study. The mean age was 53 years (range: 28-76 years). By the end of follow-up on December 1, 2024, the median observation period was 74 months (range: 10-83 months). During follow-up, 122 patients (34.5%) experienced disease progression, with a median time to progression of 36 months (range: 10-68 months). For subsequent analyses, patients were categorized into two groups based on progression status during follow-up: the progression group (n = 122) and the non-progression group (n = 232).

Clinical and pathological data

Clinical data: Patient demographic information, laboratory results, and clinical records were reviewed to document age, body mass index (BMI), menstrual status, and pre-treatment serum levels of tumor markers including carcinoembryonic antigen (CEA) and carbohydrate antigen 153 (CA153). Lymph node metastasis status was also recorded.

Pathological data: Data including Ki-67 expression, molecular subtype, and histological grade were obtained from hematoxylin-eosin (HE) staining and immunohistochemical analyses of surgical and biopsy specimens. Histological grading was conducted according to the Nottingham histological grading system [11], classifying G3 as high-grade and G1-G2 as non-high-grade. Molecular subtyping was performed based on the 2013 St. Gallen Consensus Conference criteria [12]: Luminal A subtype: Estrogen receptor (ER) and/or progesterone receptor (PR) positive, HER2 negative, and low

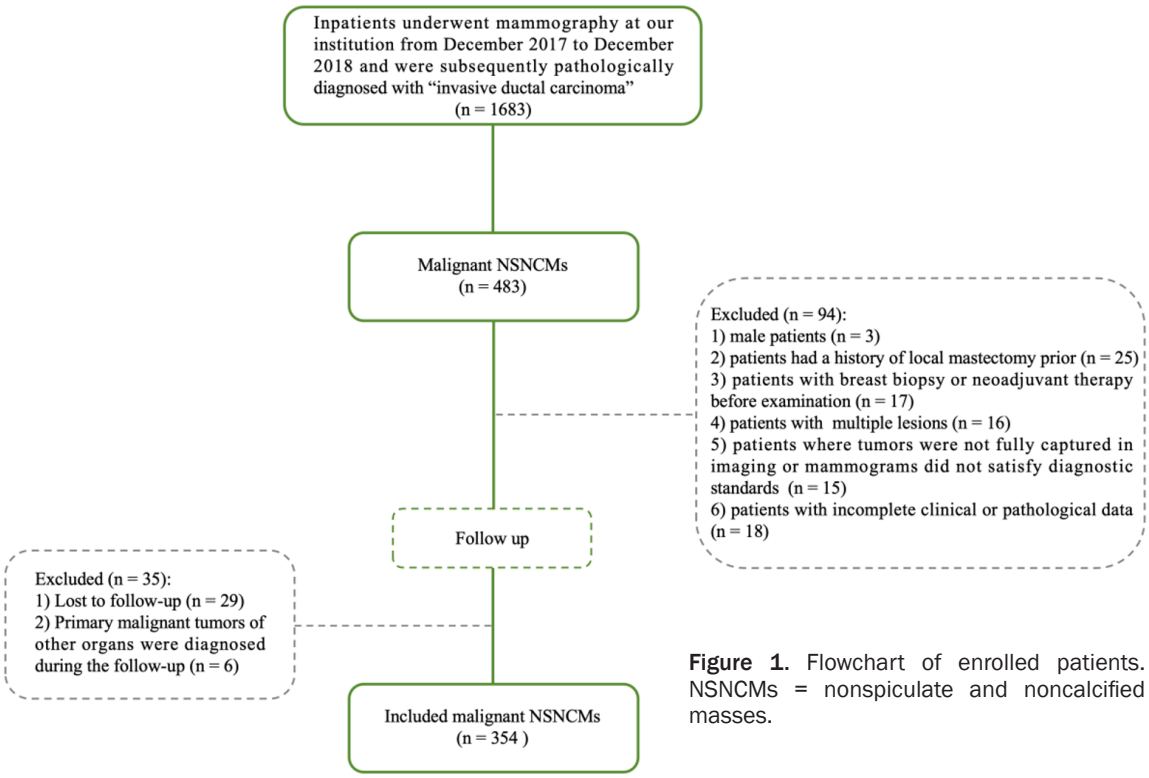

Figure 1. Flowchart of enrolled patients. NSNCMs = nonspiculate and noncalcified masses.

Ki-67 expression (< 20%); Luminal B subtype: Luminal B (HER2 negative): ER and/or PR positive, HER2 negative, high Ki-67 expression (≥ 20%); Luminal B-like (HER2 positive): ER and/or PR positive, HER2 positive (protein overexpression or gene amplification), regardless of Ki-67 expression level; HER2 overexpression subtype: HER2 positive (protein overexpression or gene amplification), ER and PR negative; Triple-negative subtype: HER2, ER, and PR all negative.

ER/PR positivity was defined as ≥ 1% nuclear staining in tumor cells [13]. HER2 status was assessed per the latest American Society of Clinical Oncology guidelines [14], with negative defined as IHC scores of 0, 1+, or 2+ with negative fluorescence in situ hybridization (FISH) results, and positive as IHC 3+ or 2+ with positive FISH results.

Mammography acquisition

Mammographic imaging was performed using full-field digital mammography systems (Fuji MS-3500, Japan; Siemens Inspiration, Germany). Trained technicians performed the examinations, utilizing automatic exposure in most cases and manual adjustment for dense or large masses. Standard cranio-caudal (CC) and medio-lateral oblique (MLO) views were obtained for each patient. Additional views such as medio-lateral (ML) or latero-medial oblique (LMO) were acquired when necessary based on mass location to ensure comprehensive evaluation. Examination pressure was adjusted through effective communication to maximize patient comfort. Images were transmitted to both the PACS and diagnostic workstations for analysis.

Imaging analysis

Three radiologists independently reviewed all mammograms on specialized diagnostic workstations with 5.8 M dual-display screens, blinded to pathological results. Initial assessments were conducted by a radiologist with 7 years of breast imaging experience, then reviewed by a deputy chief physician with 18 years of experience or a chief physician with 20 years of expertise in mammography. Discrepancies were resolved through consensus discussions among the three radiologists.

Tumor characteristics were assessed using the 2013 American College of RadiologyBreast Imaging Reporting and Data System (BI-RADS®)

Table 1. Classification of mammographic tumor signs and extratumoral signs

Mammography signs	Classification	Subclassification
Tumor signs		
	Tumor shape	
	Tumor density	
	Tumor margin	
Extratumoral signs		
	Parenchymal structural abnormalities	
		Contraction sign
		Distortion sign
		Pushing sign
		Atrophy sign
	Trabecular structural abnormalities	
		Parallel sign
		Vertical sign
		Reticular sign
	Halo sign	

lexicon [15]. Based on our prior research [10], extratumoral signs of malignant NSNCMs were systematically categorized according to BI-RADS® guidelines and our extensive breast imaging experience. Details of classification methodology are provided in **Table 1**, with illustrative examples in the Figures S1 and S2.

Follow-up

Follow-up data were obtained through hospital record review and telephone interviews. The primary endpoint was progression-free survival (PFS), defined as the time from treatment initiation to first documented disease progression or end of follow-up. PFS rate (PFS%) represented the probability of no progression within a specified period. Follow-ups were conducted every three months for the first two years and every six months thereafter, including physical examination, laboratory testing, and breast, lymph node, and abdominal ultrasonography. Annual chest CT and mammography were performed, with breast MRI, brain CT/MRI, and bone scans conducted when clinically indicated. Follow-up concluded on December 1, 2024.

Disease progression was defined based on the following criteria [16, 17]: Postoperative local recurrence or distant metastasis; Increase in size, enlargement, or appearance of new lesions at original sites; Suspicious lesions confirmed by pathology or by at least two imaging modalities, with changes consistent with clinical course (e.g. lesion shrinkage with improvement or growth with deterioration); Comprehensive clinical evaluation confirming progression.

Statistical analysis

Data were collected and organized in Excel 2010, with statistical analysis performed using SPSS 26.0. Continuous variables were reported as mean ± standard deviation (SD) after assessing normality using the Shapiro-Wilk test. For normally distributed data with homogeneous variance (verified by Levene's test), intergroup comparisons were conducted using the independent samples t-test; otherwise, the Mann-Whitney U test was used. Categorical variables were presented as percentages and analyzed using the χ^2 test.

Univariate Cox proportional hazards regression was employed to evaluate associations between clinicopathological and imaging characteristics and disease progression. Variables with $P < 0.05$ in univariate analysis were included in multivariate Cox regression. Variables remaining significant ($P < 0.05$) in multivariate analysis were identified as independent predictors. Kaplan-Meier survival curves were constructed to estimate PFS across different stratifications of these predictors.

Results

Comparison of clinicopathological data and follow-up results

Table 2 summarizes the clinicopathological characteristics of the patients. In the progres-

Table 2. Comparison of clinicopathological data

Characteristics	Total n = 354	Progression n = 122	Non-progression n = 232	t/Z/χ^2	*p*
Age (years)	52.51±10.50	53.38±10.17	52.05±10.66	-1.133	0.258
BMI	24.42±4.05	24.65±3.48	24.30±4.33	-0.769	0.442
Menopausal status				0.751	0.386
pre-menopause	165 (46.6%)	53 (43.4%)	112 (48.3%)		
post-menopause	189 (53.4%)	69 (56.6%)	120 (51.7%)		
CEA (ng/ml)	1.78 (1.20, 2.79)	1.90 (1.25, 3.01)	1.74 (1.20, 2.70)	-1.328	0.184
CA153 (U/ml)	10.51 (7.89, 15.49)	11.12 (8.24, 16.05)	10.09 (7.61, 14.74)	-1.466	0.143
Ki-67 (%)				12.675	< 0.001
< 20	61 (17.2%)	9 (7.4%)	52 (22.4%)		
≥ 20	293 (82.8%)	113 (92.6%)	180 (77.6%)		
Histological grade				28.611	< 0.001
G1-2	221 (62.4%)	53 (43.4%)	168 (72.4%)		
G3	133 (37.6%)	69 (56.6%)	64 (27.6%)		
Lymph node metastasis				27.244	< 0.001
Negative	230 (65%)	57 (46.7%)	173 (74.6%)		
Positive	124 (35%)	65 (53.3%)	59 (25.4%)		
Molecular subtypes				26.277	< 0.001
Luminal A	78 (22%)	34 (27.9%)	44 (19%)		
Luminal B	205 (57.9%)	53 (43.4%)	152 (65.5%)		
HER2 over-expression	35 (9.9%)	11 (9%)	24 (10.3%)		
Triple negative	36 (10.2%)	24 (19.7%)	12 (5.2%)		

Notes: BMI = Body Mass Index, CEA = Carcinoembryonic Antigen, CA153 = Carbohydrate Antigen 153, HER2 = human epidermal growth factor receptor 2.

sion group, 65 patients (53.3%) had lymph node metastasis, compared to 59 patients (25.4%) in the non-progression group, representing a significant difference (P < 0.001). Regarding histological grade, 69 patients (56.6%) in the progression group were diagnosed as G3, while most patients in the non-progression group were G1-2 (168 patients, 72.4%), also showing a significant difference (P < 0.001). In terms of molecular subtypes, the progression group had a significantly higher proportion of triple-negative breast cancer than the non-progression group (19.7% vs. 5.2%, P < 0.001). Additionally, Ki-67 expression differed significantly between the two groups (P < 0.001). However, no significant differences were observed in age, BMI, or other clinicopathological factors (all P > 0.05).

Comparison of mammographic signs

As shown in **Table 3**, among tumor signs, only tumor length showed a significant difference between the two groups (P < 0.001), while no significant differences were found in tumor shape, density, or margins (all P > 0.05).

Notably, extratumoral parenchymal and trabecular structural abnormalities differed significantly between groups (P < 0.05). Specifically, 81.1% of patients in the progression group exhibited extratumoral parenchymal structural abnormalities, compared to 63.8% in the non-progression group. Similarly, extratumoral trabecular structural abnormalities were present in 85.2% of patients in the progression group versus 71.6% in the non-progression group. No significant difference was observed for the extratumoral halo sign (P > 0.05).

Cox univariate and multivariate analyses

Table 4 presents the results of Cox univariate and multivariate analyses. In univariate analysis, histological grade, lymph node metastasis, molecular subtype, and Ki-67 expression were significantly associated with disease progression. However, in multivariate analysis, only

Table 3. Comparison of mammographic data

Characteristics	Total n = 354	Progression n = 122	Non-progression n = 232	Z/χ^2	*p*
Tumor length (mm)	20.50 (16.00, 27.25)	23.00 (17.00, 30.25)	19.00 (15.00, 26.00)	-3.523	< 0.001
Tumor shape				1.836	0.175
Round/Oval	251 (70.9%)	81 (66.4%)	170 (73.3%)		
Irregular	103 (29.1%)	41 (33.6%)	62 (26.7%)		
Tumor density				1.077	0.299
Low/Equal	50 (14.1%)	14 (11.5%)	36 (15.5%)		
High	304 (85.9%)	108 (88.5%)	196 (84.5%)		
Tumor margin				0.009	0.925
Circumscribed/Obscured	15 (4.2%)	5 (4.1%)	10 (4.3%)		
Indistinct	339 (95.8%)	117 (95.9%)	222 (95.7%)		
Parenchyma				11.418	0.001
Negative	107 (30.2%)	23 (18.9%)	84 (36.2%)		
Positive	247 (69.8%)	99 (81.1%)	148 (63.8%)		
Trabecula				8.285	0.004
Negative	84 (23.7%)	18 (14.8%)	66 (28.4%)		
Positive	270 (76.3%)	104 (85.2%)	166 (71.6%)		
Halo Sign				0.000	0.992
Negative	232 (65.5%)	80 (65.6%)	152 (65.5%)		
Positive	122 (34.5%)	42 (34.4%)	80 (34.5%)		

Table 4. Cox regression analysis of predictors of disease progression in malignant NSNCMs

Characteristics		Univariate analysis			Multivariate analysis		
		HR	95% CI	*p*	HR	95% CI	*p*
Age (years)		1.01	1.00-1.03	0.169			
BMI		1.02	0.97-1.06	0.416			
Menopausal status		1.21	0.84-1.73	0.303			
CEA (ng/ml)		1.03	1.00-1.07	0.053			
CA153 (U/ml)		1.00	0.98-1.02	0.933			
Histological grade		2.29	1.46-3.61	< 0.001	2.03	1.05-3.92	0.036
Lymph node metastasis		2.50	1.75-3.57	< 0.001	2.37	1.64-3.42	< 0.001
Molecular subtypes	Luminal A	1.00		< 0.001	1.00		0.324
	Luminal B	0.50	0.32-0.77	0.002	0.88	0.53-1.45	0.622
	HER2 over-expression	0.60	0.31-1.19	0.146	0.97	0.47-1.99	0.936
	Triple negative	2.10	1.25-3.55	0.005	1.49	0.87-2.56	0.144
Ki-67 (%)		3.14	1.59-6.20	0.001	1.48	0.71-3.09	0.290
Tumor length (mm)		1.01	1.00-1.02	0.003	1.01	1.00-1.02	0.067
Tumor shape		1.31	0.90-1.91	0.154			
Tumor density		1.24	0.71-2.16	0.448			
Tumor margin		0.97	0.40-2.38	0.950			
Contraction Sign		2.78	1.95-3.99	< 0.001	2.56	1.60-4.09	< 0.001
Distortion Sign		1.52	1.04-2.21	0.030	1.48	0.87-2.53	0.145
Pushing Sign		1.61	0.66-3.95	0.295			
Atrophy Sign		1.14	0.72-1.81	0.572			
Parallel Sign		2.95	1.98-4.39	< 0.001	2.71	1.57-4.70	< 0.001
Vertical Sign		0.79	0.55-1.14	0.208			
Reticular Sign		2.17	1.32-3.58	0.002	1.14	0.57-2.28	0.705
Halo Sign		1.00	0.69-1.46	0.981			

Notes: BMI = Body Mass Index, CEA = Carcinoembryonic Antigen, CA153 = Carbohydrate Antigen 153, HER2 = human epidermal growth factor receptor 2, HR = Hazard ratio, CI = Confidence Interval.

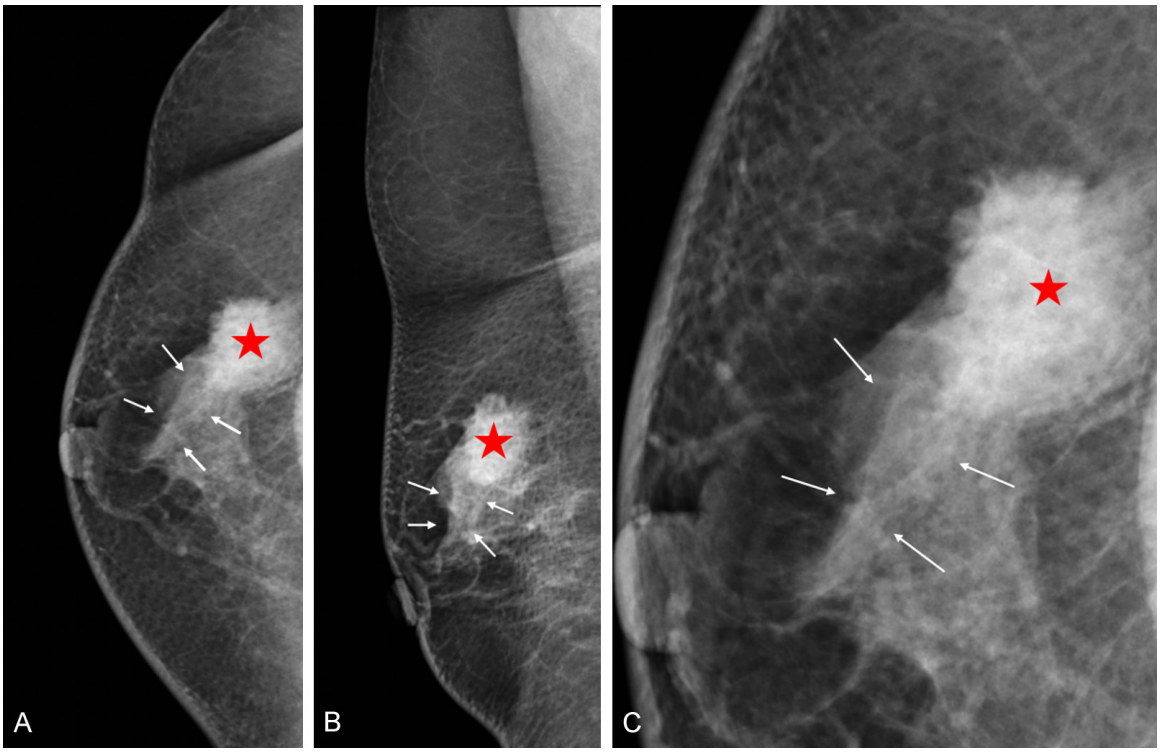

Figure 2. Example of a patient with extratumoral parenchymal contraction sign. A 54-year-old woman was diagnosed with invasive ductal carcinoma grade III, without lymph node metastasis and classified as the Luminal B subtype. Disease progression was noted 27 months post-treatment. Mammography images in the CC (A) and MLO (B) views showed a mass located in the upper outer quadrant of the right breast (marked by a red star). The margin of the mass appeared indistinct and was not associated with spiculation or calcification, leading to its classification as NSNCM. The presence of parenchymal contraction sign (C, marked with a white arrow and a "wedge" contraction of the extramural parenchyma) observed anterior to the mass may indicate an unfavorable prognosis. CC = cranio-caudal, MLO = medio-lateral oblique, NSNCM = nonspiculate and noncalcified mass.

lymph node metastasis [hazard ratio (HR) = 2.37, 95% confidence interval (CI): 1.64-3.42, P < 0.001] and histological grade (HR = 2.03, 95% CI: 1.05-3.92, P = 0.036) remained as independent predictors of malignant NSNCM progression.

For tumor signs, only tumor length was significantly associated with progression in univariate analysis (HR = 1.01, 95% CI: 1.00-1.02, P = 0.003), but this association did not persist in multivariate analysis. Several extratumoral signs were associated with disease progression in univariate analysis, including the contraction and distortion signs in parenchymal structural abnormalities and the parallel and reticular signs in trabecular structural abnormalities. After multivariate adjustment, the contraction sign (HR = 2.56, 95% CI: 1.60-4.09, P < 0.001) and parallel sign (HR = 2.71, 95% CI: 1.57-4.70, P < 0.001) were confirmed as independent predictors, demonstrating strong prognostic value. **Figures 2** and **3** show mammographic images from two patients exhibiting these extratumoral structural abnormalities.

Kaplan-Meier survival analysis

Kaplan-Meier survival curves were constructed with PFS on the x-axis and PFS% on the y-axis. **Figure 4** presents survival curves stratified by lymph node metastasis, histological grade, contraction sign, and parallel sign. The results demonstrate that patients with contraction or parallel signs exhibited a more rapid decline in PFS compared to those without these signs, indicating faster disease progression and shorter PFS durations.

Similarly, patients with lymph node metastasis showed a steeper decline in survival compared to those without metastasis. Patients with G3 histological grade also demonstrated a more rapid decrease in PFS compared to patients with G1 or G2 grades.

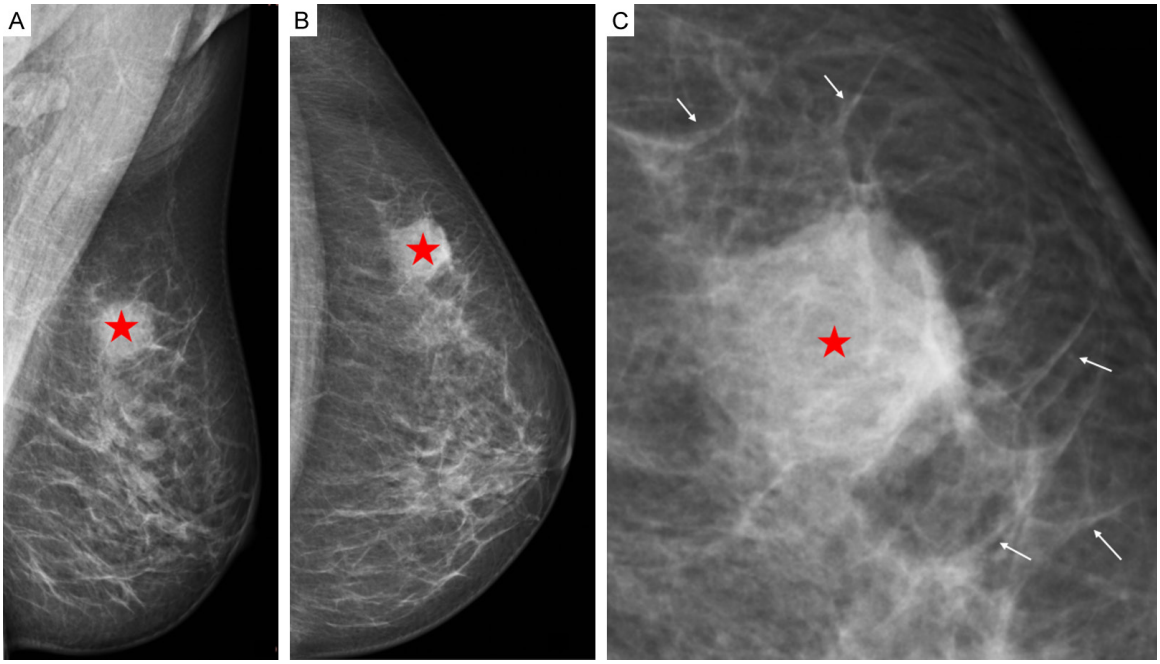

Figure 3. Example of a patient with extratumoral parallel trabecular sign. A 67-year-old female patient was diagnosed with grade II invasive ductal carcinoma, accompanied by lymph node metastasis and classified as TNBC. Disease progression was noted 18 months post-treatment. Mammography images in the MLO (A) and CC (B) views showed a mass located in the upper outer quadrant of the left breast (marked by a red star). The mass was categorized as NSNCM due to its indistinct margin, absence of spiculation, and lack of calcification. The presence of multiple thickened breast trabecular parallel to the mass, referred to as the parallel trabecular sign (C, marked with white arrows), is indicative of a potentially unfavorable prognosis. TNBC = triple-negative breast cancer, CC = craniocaudal, MLO = medio-lateral oblique, NSNCM = nonspiculate and noncalcified mass.

Discussion

In this study, we investigated the association between extratumoral signs on mammography and breast cancer prognosis in patients with malignant NSNCMs. We found that certain extratumoral signs, specifically the contraction sign and parallel trabecular sign, outperformed conventional clinicopathological features in predicting prognosis, serving as independent risk stratification markers for malignant NSNCMs.

Consistent with previous studies [18-20], our findings demonstrated that lymph node metastasis (HR = 2.37, 95% CI: 1.64-3.42, P < 0.001) and histological grade (HR = 2.03, 95% CI: 1.05-3.92, P = 0.036) were independent predictors of disease progression in malignant NSNCMs. Lymph node involvement indicates the tumor's capacity for lymphatic invasion, which is biologically associated with elevated levels of pro-migratory molecules, such as matrix metalloproteinases, that facilitate metastasis to lymph nodes [21]. Thus, lymph node metastasis often signals a higher risk of distant recurrence. Additionally, higher histological grades (e.g., Bloom-Richardson grade III) reflect increased cellular atypia, mitotic activity, and genomic instability, correlating with rapid tumor growth and worse prognosis [22].

Clinically, triple-negative breast cancer (TNBC) is widely recognized as a highly aggressive subtype due to its receptor-negative status and limited therapeutic options [23, 24]. However, our findings diverged from this consensus. Although univariate analysis indicated a trend, TNBC did not retain significance in multivariate models. This discrepancy may be attributable to the small number of TNBC cases (36 patients) and potential confounding by imaging features linked to TNBC biology, such as TP53 mutations associated with contraction signs [25]. Larger studies are required to validate whether these extratumoral signs specifically impact TNBC prognosis.

In contrast to previous studies [26-28], age and Ki-67 expression were not significant predic-

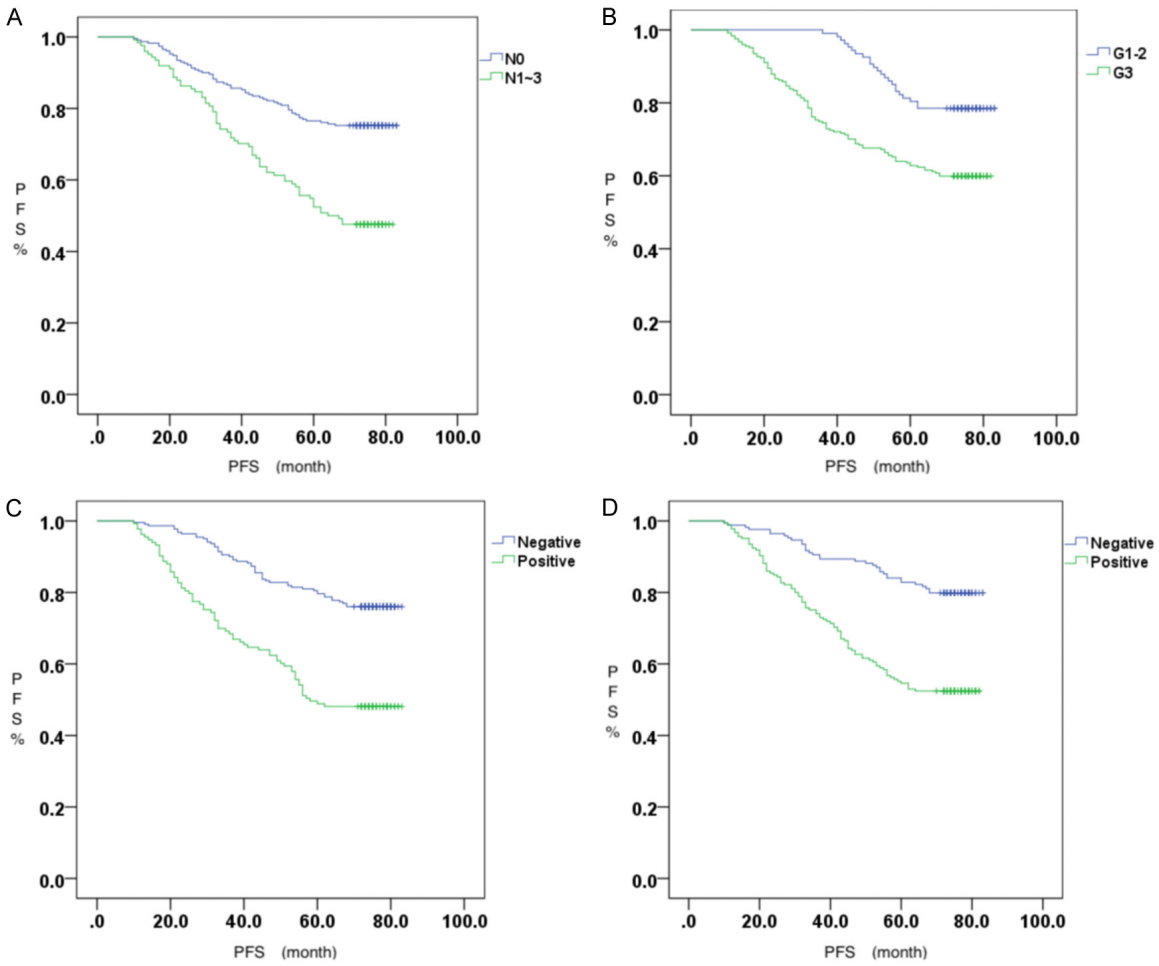

Figure 4. Kaplan-Meier survival curves based on four independent predictors. A. Lymph node metastasis. B. Histological grade. C. Extratumoral parenchymal contraction sign. D. Extratumoral parallel trabecular sign. Patients with lymph node metastasis, G3 histological grade, contraction sign or parallel trabecular sign (indicated by the green line), exhibit a more rapid decline in the survival curve compared to those corresponding groups (indicated by the blue line). This suggests that these patients experience accelerated disease progression and a shorter progression-free survival (PFS).

tors in our cohort. This may be related to the unique biology of NSNCMs, such as slower proliferation rates or age-related stromal fibrosis, or due to single-center selection bias, underscoring the need for multicenter validation.

Breast cancer is highly heterogeneous; even patients with identical pathological or molecular subtypes can exhibit markedly different outcomes [29]. Consequently, there is a growing need for additional objective indicators to comprehensively assess breast cancer prognosis. The peritumoral microenvironment, a critical driver of tumor progression, has substantial prognostic potential [30-32]. Distinct microenvironmental characteristics inevitably manifest as specific features on mammography.

Previous studies examining mammographic signs and breast cancer prognosis have predominantly focused on tumor characteristics [33], such as mass size and density, or on breast calcifications [34]. However, few studies have explored the prognostic significance of extratumoral structural abnormalities, particularly in NSNCMs. In our analysis, conventional tumor signs showed no significant predictive power for disease progression in malignant NSNCMs. Conversely, two extratumoral signs emerged as independent predictors, underscoring their unique value in risk assessment. This finding highlights the superior prognostic utility of extratumoral signs in evaluating malignant NSNCMs.

In this study, approximately one-third of malignant NSNCMs exhibited the extratumoral contraction sign. This sign manifests as band-like or wedge-shaped contraction of the extratumoral or quadrant parenchyma, or as retraction of tumor margins. The most direct cause of this contraction is likely the fibrotic elastic response surrounding the ducts [35, 36]. This fibrosis is driven by transforming growth factor-β (TGF-β) and platelet-derived growth factor (PDGF), creating a stiff microenvironment that promotes tumor cell migration via integrin and YAP/TAZ signaling pathways [37-39]. Fibrotic stroma is associated with poorer survival outcomes, particularly in TNBC [40].

The tumor microenvironment not only alters the extratumoral parenchyma but also induces abnormalities in trabecular structures. In our study, the parallel trabecular sign - defined as approximately parallel trabeculae surrounding or distant from the mass, potentially located in deep or subcutaneous fat layers - was identified as an independent predictor of malignant NSNCM progression (HR = 2.71, 95% CI: 1.57-4.70, $P < 0.001$). This sign is considered to be associated with interstitial edema and lymphatic dilation [41]. Peritumoral edema, indicative of increased vascular permeability or inflammatory responses, suggests a heightened risk of tumor invasion and early metastasis. Edematous regions often harbor hypoxic tumor cells, which upregulate HIF-1α and promote epithelial-mesenchymal transition (EMT), thereby enhancing metastatic potential [42].

Our findings further indicate that the presence of the contraction sign or parallel trabecular sign holds significant value for risk stratification in malignant NSNCMs. Specifically, patients exhibiting these signs experienced a more rapid decline in PFS%, faster disease progression, and shorter progression-free survival times.

Moreover, the identified independent predictors may synergistically influence tumor progression. Fibrotic contraction (contraction sign) and lymphatic dilation (parallel sign) both result from tumor microenvironment remodeling. Fibroblasts secrete vascular endothelial growth factor and PDGF, promoting lymphangiogenesis and edema, while stiff collagen matrices enhance tumor cell motility. This cycle accelerates local invasion and lymph node metastasis [43]. Metastatic cells further secrete factors that induce stromal fibrosis and edema, amplifying the contraction and parallel signs.

Clinically, combining histological features with imaging signs (e.g., contraction and parallel signs) improves risk stratification [44]. For example, patients with malignant NSNCMs exhibiting extratumoral parenchymal contraction or parallel trabecular signs along with high-grade histology or lymph node metastasis may have a poor prognosis and could benefit from multimodal therapy, such as neoadjuvant chemotherapy combined with anti-angiogenic agents [45]. Conversely, the absence of these signs suggests a favorable prognosis, helping to avoid overtreatment, reduce side effects and costs, and extend follow-up intervals.

This study has several limitations. First, it is a single-center retrospective analysis, introducing potential selection bias and uneven distribution of molecular subtypes, such as small sample sizes for HER2-overexpressing (35 patients) and triple-negative subtypes (36 patients) among the 354 enrolled. This imbalance may limit the generalizability of our conclusions to these subtypes, affecting the external validity of the study. Second, evaluation of mammographic signs relied on visual assessment, which requires observer expertise and may lead to interobserver variability. Moreover, visual assessment is inherently subjective and lacks objective validation methods, potentially introducing human-related bias into the results.

Given these limitations, future studies should aim to reduce bias by increasing sample sizes, implementing multicenter data collection, and ensuring diverse regional representation. Tertiary hospitals from different regions will be selected, and collaborating centers must meet strict criteria, including ethical approvals, standardized imaging and examination protocols, and comprehensive pathological documentation. Standardized protocols for image acquisition, clinical data recording, and imaging assessment will enhance consistency. Additionally, incorporating artificial intelligence to automate regions of interest segmentation and develop prognostic models may improve objectivity and reproducibility.

In conclusion, based on the extratumoral sign classification established in our preliminary

study, we determined that subclassifications of extratumoral structural abnormalities hold significant predictive value for the prognosis of malignant NSNCMs. Therefore, continuous monitoring of these extratumoral signs identified on mammography is recommended for patients diagnosed with malignant NSNCMs.

Acknowledgements

This work was partially funded by the Haiyan Funds of Harbin Medical University Cancer Hospital (JJQN2023-14).

Disclosure of conflict of interest

None.

Address correspondence to: Xiushi Zhang and Jianghong Sun, Department of Radiology, Harbin Medical University Cancer Hospital, No. 150 Haping Road, Harbin 150081, Heilongjiang, China. Tel: +86-15945058456; E-mail: xiushiz@126.com (XSZ); Tel: +86-13936515138; E-mail: jianghong713@sina.cn (JHS)

References

[1] Cao W, Qin K, Li F and Chen W. Comparative study of cancer profiles between 2020 and 2022 using global cancer statistics (GLOBOCAN). J Natl Cancer Cent 2024; 4: 128-134.

[2] Siegel RL, Giaquinto AN and Jemal A. Cancer statistics, 2024. CA Cancer J Clin 2024; 74: 12-49.

[3] Lee SE, Ahn SG, Ji JH, Kook Y, Jang JS, Baek SH, Jeong J and Bae SJ. Optimal treatment strategy for hormone receptor-positive human epidermal growth factor receptor 2-negative breast cancer patients with 1-2 suspicious axillary lymph node metastases on breast magnetic resonance imaging: upfront surgery vs. neoadjuvant chemotherapy. Front Oncol 2023; 13: 936148.

[4] Huang Longcoy LT, Tai CY, Longcoy J, Huei-Yu Wang J, Yin J, Cowan L and Sullivan KL. Effects of educational interventions in facilitating mammography screening among Asian American women: a meta-analysis. Oncol Nurs Forum 2023; 50: 263-272.

[5] Abu Abeelh E and AbuAbeileh Z. Impact of mammography screening frequency on breast cancer mortality rates. Cureus 2023; 15: e49066.

[6] Tommasino N, Feo F, Cantelli M and Fattore D. Cutaneous signs of breast cancer: when a dermatologic evaluation is useful after a negative mammography. Dermatol Pract Concept 2024; 14: e2024180.

[7] Wang J, Zhao L, Hu X, Lv L, Zhang X, Lu M and Hu G. Clinicopathological characteristics and prognostic significance of casting-type calcifications in patients with invasive breast cancer presenting with microcalcification. Sci Rep 2024; 14: 13351.

[8] Bhatia M, Ahmed R, Nagarajakumar A, Alani A, Doddi S and Metafa A. Measurement of malignant spiculated mass lesions on mammogram: do we include the length of the spicules? J Cancer Res Ther 2023; 19: 1794-1796.

[9] Ryu MJ, Kim YS and Lee SE. Association between imaging features using the BI-RADS and tumor subtype in patients with invasive breast cancer. Curr Med Imaging 2022; 18: 648-657.

[10] Xu Y, Sun J, Guo F, Nanding A, Li Q and Jiang D. Focus on the predictive value of subclassification of extratumoral structural abnormalities for malignant nonspiculate and noncalcified masses on digital mammography. Front Genet 2022; 13: 822858.

[11] Benitez Fuentes JD, Morgan E, de Luna Aguilar A, Mafra A, Shah R, Giusti F, Vignat J, Znaor A, Musetti C, Yip CH, Van Eycken L, Jedy-Agba E, Pineros M and Soerjomataram I. Global stage distribution of breast cancer at diagnosis: a systematic review and meta-analysis. JAMA Oncol 2024; 10: 71-78.

[12] Goldhirsch A, Winer EP, Coates AS, Gelber RD, Piccart-Gebhart M, Thurlimann B, Senn HJ and Panel M. Personalizing the treatment of women with early breast cancer: highlights of the St Gallen International Expert Consensus on the Primary Therapy of Early Breast Cancer 2013. Ann Oncol 2013; 24: 2206-2223.

[13] Allison KH, Hammond MEH, Dowsett M, McKernin SE, Carey LA, Fitzgibbons PL, Hayes DF, Lakhani SR, Chavez-MacGregor M, Perlmutter J, Perou CM, Regan MM, Rimm DL, Symmans WF, Torlakovic EE, Varella L, Viale G, Weisberg TF, McShane LM and Wolff AC. Estrogen and progesterone receptor testing in breast cancer: ASCO/CAP guideline update. J Clin Oncol 2020; 38: 1346-1366.

[14] Varga Z and Noske A. Impact of modified 2013 ASCO/CAP guidelines on HER2 testing in breast cancer. One year experience. PLoS One 2015; 10: e0140652.

[15] American College of R. ACR BI-RADS atlas: breast imaging reporting and data system. Reston, VA: American College of Radiology, 2013.

[16] Breast Cancer Expert Committee of National Cancer Quality Control Center; Health Management Professional Committee of Beijing Breast Cancer Prevention and Control Society. [Comprehensive management guideline for

breast cancer follow-up and healthcare (2022 edition)]. Zhonghua Zhong Liu Za Zhi 2022; 44: 1-28.
[17] Expert Panel on Breast Imaging, McDonald ES, Scheel JR, Lewin AA, Weinstein SP, Dodelzon K, Dogan BE, Fitzpatrick A, Kuzmiak CM, Newell MS, Paulis LV, Pilewskie M, Salkowski LR, Silva HC, Sharpe RE Jr, Specht JM, Ulaner GA and Slanetz PJ. ACR Appropriateness Criteria(R) imaging of invasive breast cancer. J Am Coll Radiol 2024; 21: S168-S202.
[18] Teng L, Du J, Yan S, Xu P, Liu J, Zhao X and Tao W. A novel nomogram and survival analysis for different lymph node status in breast cancer based on the SEER database. Breast Cancer 2024; 31: 769-786.
[19] Liu R, Chen J, Cao W, Li T, Liao Y and Li Y. Risk factors and prognosis of sentinel lymph node metastasis in breast-conserving breast cancer: a retrospective study based on the SEER database. Medicine (Baltimore) 2024; 103: e37263.
[20] van Dooijeweert C, van Diest PJ, Baas IO, van der Wall E and Deckers IA. Variation in breast cancer grading: the effect of creating awareness through laboratory-specific and pathologist-specific feedback reports in 16 734 patients with breast cancer. J Clin Pathol 2020; 73: 793-799.
[21] Pan Y, Zou Q, Yin W, Huang Z, Zhao Y, Mo Z, Li L and Yang J. Development of lymph node metastasis-related prognostic markers in breast cancer. J Proteomics 2024; 291: 105045.
[22] Wang X, Liu S and Xue Y. Clinicopathological features and prognosis of male breast cancer. J Int Med Res 2021; 49: 3000605211049977.
[23] You YH, Kim MK and Lee JY. Prognosis and adjusting factors in elderly patients with triple-negative breast cancer: comparing with young and middle age groups. Clin Breast Cancer 2024; 24: e258-e265.
[24] Acevedo F, Walbaum B, Medina L, Merino T, Camus M, Puschel K, Ramirez K, Manzor M, Veglia P, Martinez R, Guerra C, Navarro M, Bauerle C, Dominguez F and Sanchez C. Clinical characteristics, risk factors, and outcomes in Chilean triple negative breast cancer patients: a real-world study. Breast Cancer Res Treat 2023; 197: 449-459.
[25] Bardia A, Rugo HS, Tolaney SM, Loirat D, Punie K, Oliveira M, Brufsky A, Kalinsky K, Cortes J, Shaughnessy JO, Dieras V, Carey LA, Gianni L, Piccart-Gebhart M, Loibl S, Yoon OK, Pan Y, Hofsess S, Phan SC and Hurvitz SA. Final results from the randomized phase III ASCENT clinical trial in metastatic triple-negative breast cancer and association of outcomes by human epidermal growth factor receptor 2 and trophoblast cell surface antigen 2 expression. J Clin Oncol 2024; 42: 1738-1744.
[26] Yang Y, Wei W, Jin L, He H, Wei M, Shen S, Pi H, Liu Z, Li H and Liu J. Comparison of the characteristics and prognosis between very young women and older women with breast cancer: a multi-institutional report from China. Front Oncol 2022; 12: 783487.
[27] Koon Sun Pat M, Manraj M and Manraj S. Breast cancer survival analysis in the republic of mauritius by age, stage at diagnosis and molecular subtype: a retrospective cohort study. Int J Cancer 2025; 156: 331-338.
[28] Ma Q, Liu YB, She T and Liu XL. The role of Ki-67 in HR+/HER2- breast cancer: a real-world study of 956 patients. Breast Cancer (Dove Med Press) 2024; 16: 117-126.
[29] Whitworth PW, Beitsch PD, Pellicane JV, Baron PL, Lee LA, Dul CL, Murray MK, Gittleman MA, Budway RJ, Rahman RL, Kelemen PR, Dooley WC, Rock DT, Cowan KH, Lesnikoski BA, Barone JL, Ashikari AY, Dupree BB, Wang S, Menicucci AR, Yoder EB, Finn C, Corcoran K, Blumencranz LE, Audeh W and Group NI. Distinct neoadjuvant chemotherapy response and 5-year outcome in patients with estrogen receptor-positive, human epidermal growth factor receptor 2-negative breast tumors that reclassify as basal-type by the 80-gene signature. JCO Precis Oncol 2022; 6: e2100463.
[30] Dzobo K, Senthebane DA and Dandara C. The tumor microenvironment in tumorigenesis and therapy resistance revisited. Cancers (Basel) 2023; 15: 376.
[31] Dominguez-Cejudo MA, Gil-Torralvo A, Cejuela M, Molina-Pinelo S and Salvador Bofill J. Targeting the tumor microenvironment in breast cancer: prognostic and predictive significance and therapeutic opportunities. Int J Mol Sci 2023; 24: 16771.
[32] Rodriguez-Bejarano OH, Parra-Lopez C and Patarroyo MA. A review concerning the breast cancer-related tumour microenvironment. Crit Rev Oncol Hematol 2024; 199: 104389.
[33] Moshina N, Backmann HA, Skaane P and Hofvind S. Mammographic features and risk of breast cancer death among women with invasive screen-detected cancer in BreastScreen Norway 1996-2020. Eur Radiol 2024; 34: 3364-3374.
[34] Evans A, Sim YT, Whelehan P, Savaridas S, Jordan L and Thompson A. Are baseline mammographic and ultrasound features associated with metastasis free survival in women receiving neoadjuvant chemotherapy for invasive breast cancer? Eur J Radiol 2021; 141: 109790.
[35] Yombo DJK, Madala SK, Vemulapalli CP, Ediga HH and Hardie WD. Pulmonary fibroelastosis - a review. Matrix Biol 2023; 124: 1-7.
[36] Sturesdotter L, Larsson AM, Zackrisson S and Sartor H. Investigating the prognostic value of

mammographic breast density and mammographic tumor appearance in women with invasive breast cancer: the Malmo diet and cancer study. Breast 2023; 70: 8-17.
[37] Kazakova AN, Lukina MM, Anufrieva KS, Bekbaeva IV, Ivanova OM, Shnaider PV, Slonov A, Arapidi GP and Shender VO. Exploring the diversity of cancer-associated fibroblasts: insights into mechanisms of drug resistance. Front Cell Dev Biol 2024; 12: 1403122.
[38] Afshar K, Sanaei MJ, Ravari MS, Pourbagheri-Sigaroodi A and Bashash D. An overview of extracellular matrix and its remodeling in the development of cancer and metastasis with a glance at therapeutic approaches. Cell Biochem Funct 2023; 41: 930-952.
[39] Luo J, Zou H, Guo Y, Tong T, Chen Y, Xiao Y, Pan Y and Li P. The oncogenic roles and clinical implications of YAP/TAZ in breast cancer. Br J Cancer 2023; 128: 1611-1624.
[40] Faget DV and Stewart SA. Stress response regulates cancer fibroblasts. Nat Cell Biol 2022; 24: 812-814.
[41] Liu Z, Li R, Liang K, Chen J, Chen X, Li X, Li R, Zhang X, Yi L and Long W. Value of digital mammography in predicting lymphovascular invasion of breast cancer. BMC Cancer 2020; 20: 274.
[42] El-Tanani M, Rabbani SA, Babiker R, Rangraze I, Kapre S, Palakurthi SS, Alnuqaydan AM, Aljabali AA, Rizzo M, El-Tanani Y and Tambuwala MM. Unraveling the tumor microenvironment: insights into cancer metastasis and therapeutic strategies. Cancer Lett 2024; 591: 216894.
[43] Monteran L, Zait Y and Erez N. It's all about the base: stromal cells are central orchestrators of metastasis. Trends Cancer 2024; 10: 208-229.
[44] Sotodosos-Alonso L and Del Pozo MA. Cancer cell invasion: caveolae and invadosomes are partners in crime. Curr Biol 2024; 34: R244-R246.
[45] Jansson M, Lindberg J, Rask G, Svensson J, Billing O, Nazemroaya A, Berglund A, Warnberg F and Sund M. Stromal type I collagen in breast cancer: correlation to prognostic biomarkers and prediction of chemotherapy response. Clin Breast Cancer 2024; 24: e360-e369, e364.

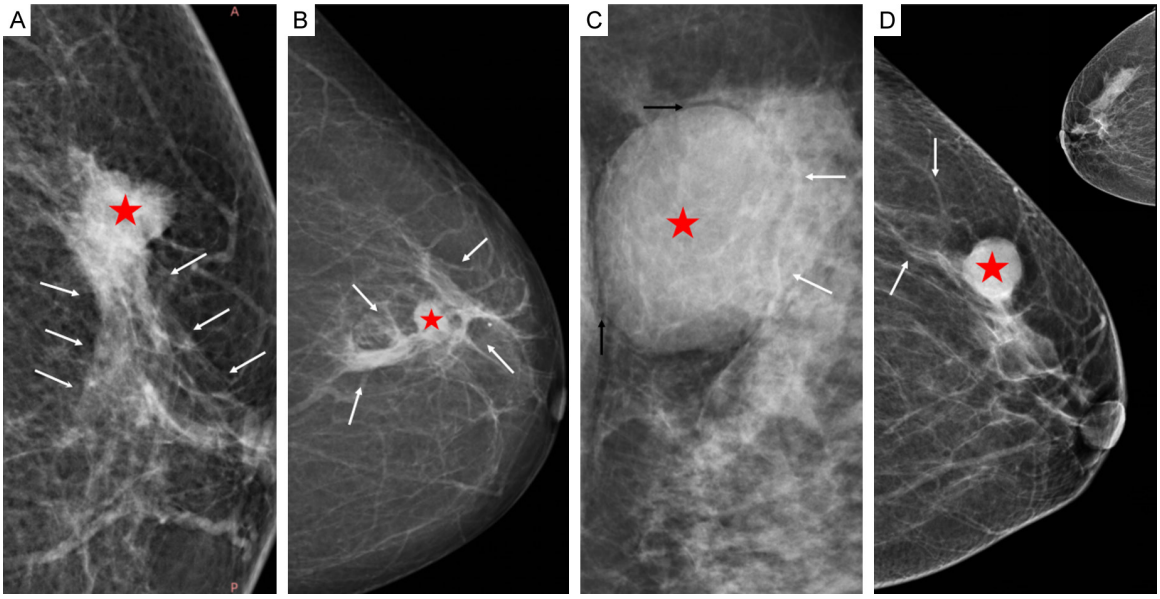

Figure S1. Subclassification of extratumoral parenchymal abnormalities. A. A mass (red star) with extratumoral parenchyma contraction sign (white arrow). B. A mass (red star) with extratumoral parenchyma distortion sign (white arrow). C. A mass (red star) with extratumoral parenchyma pushing sign (white arrow) and halo sign (black arrow). D. A mass (red star) with extratumoral parenchyma atrophy sign (white arrow), the image of the contralateral breast is shown in the upper-right corner.

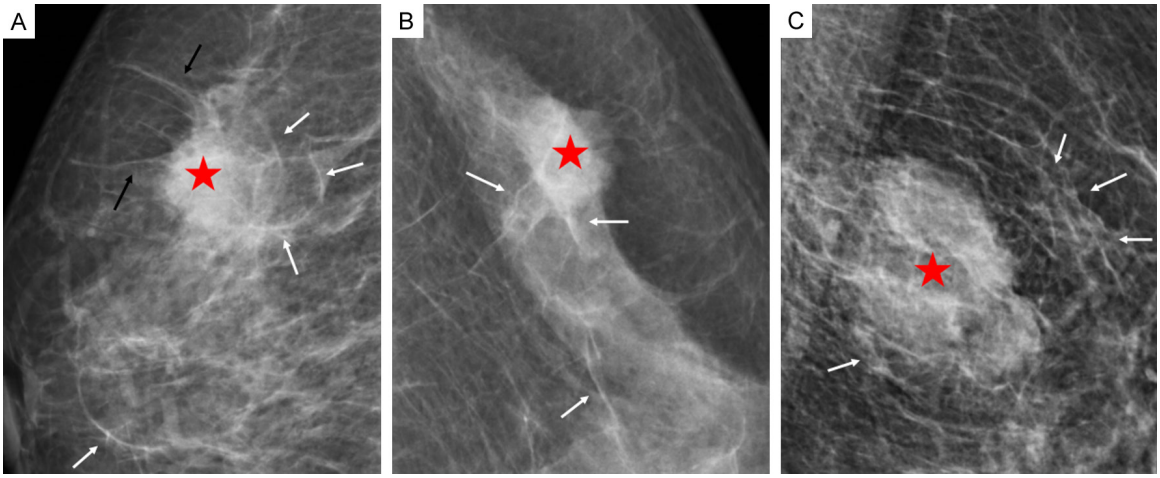

Figure S2. Subclassification of extratumoral trabecular abnormalities. A. A mass (red star) with extratumoral parallel trabecula sign (white arrow) and vertical trabecula sign (black arrow). B. A mass (red star) with extratumoral vertical trabecula sign (white arrow). C. A mass (red star) with extratumoral reticular trabecula sign (white arrow).